# Dynamic characteristics optimization of elastomer for resistance strain force sensor

*Si Chen and Haoran Lv*
Engineering Technology Center, Beijing Changcheng Institute of Metrology and Measurement, Beijing, China
*Yinming Zhao*
Beijing Changcheng Institute of Metrology and Measurement, Beijing, China, and
*Minning Wang*
Key Laboratory of Micro/Nano Systems for Aerospace of Ministry of Education, Northwestern Polytechnical University, Xian, China

**Abstract**

**Purpose** – This paper aims to provide a new method to study and improve the dynamic characteristics of the four-column resistance strain force sensor through the elastomer structure design and optimization.

**Design/methodology/approach** – Based on the mechanism analysis method, the authors first present a dynamic characteristic model of the four-column resistance strain force sensors' elastomer. Then, the authors verified and modified the model according to the Solidworks finite element simulation results. Finally, the authors designed and optimized two types of four-column elastomers based on the dynamic characteristic model and verified the improvement of sensor dynamic performance through a hammer knock dynamic experiment.

**Findings** – The Solidworks finite element simulation and hammer knock dynamic experiment results show that the relative error of the model is less than 10%, which confirms the accuracy of the model. The dynamic performance of the sensors based on the model can be improved by more than 30%, which is a great improvement in sensor dynamic performance.

**Originality/value** – The authors first present a dynamic characteristic model of the four-column elastomer and optimize the four-column sensors successfully based on the mechanism analysis method. And a new method to study and improve the dynamic characteristics of the resistance is provided.

**Keywords** Dynamic characteristics, Natural frequency, Force Sensor, Four-column elastomer, Mechanism analysis method

**Paper type** Technical paper

## 1 Introduction

Modern sensor technology includes the development of sensitive materials (Tang *et al.*, 2011; Ye *et al.*, 2001), sensor design (De Vries, 2018; Zhou *et al.*, 2013; Zhou and Luo, 2015; Ding, 2011), manufacture (XXXX, 2019; De Vries, 2018; Tang, 2016) and applications (Mu *et al.*, 2020; Tang and Huo, 2020; Zhao, 2020), sensor technology has been widely used in industrial production (Cai, 2019; Sheng and Huang, 2014), environmental protection (Ma *et al.*, 2018), resource investigation, medical diagnosis (Guo and Zhang, 2017), bioengineering, ocean exploration (Wu *et al.*, 2020), aerospace, space exploration and other fields.

The column sensor often has the best comprehensive performance among the resistance strain force sensors (Zhang *et al.*, 2012). Therefore, the four-column sensor is selected as the representative of the resistance strain force sensor to study the dynamic characteristic optimization method and related technology. The elastomer of four-column resistance strain force sensor is called four-column elastomer. The four-column elastomer has the greatest impact on the dynamic characteristics (Zhao *et al.*, 2017). Natural frequency is the primary index for the study of system dynamic characteristics, which is generally accepted in the international research field (Xu *et al.*, 2014; Li *et al.*, 2017; Yang *et al.*, 2017). Establishing a complete and accurate natural frequency model of four-column elastomer is the core and foundation of optimizing the dynamic characteristics of four-column sensor based on the above analysis.

The research of this subject is conducive to the development of four-column sensors in the dynamic measurement field and fills the gap in the dynamic characteristics design theory of resistance strain force sensors.

The current issue and full text archive of this journal is available on Emerald Insight at: **https://www.emerald.com/insight/0260-2288.htm**

Sensor Review
44/4 (2024) 405–413
Emerald Publishing Limited [ISSN 0260-2288]
[DOI 10.1108/SR-02-2022-0067]



Received 7 February 2022
Revised 27 December 2022
27 January 2023
Accepted 15 February 2023

Researchers have proposed and applied the principle of force sensor optimization design to solve the optimal structural parameters. Chen improved the structural stiffness of the sensor to 3,000 N/m (Chen and Yuan, 1997); Wu improved the sensor sensitivity to $1.64 \times 10^{-3}$ (Wu *et al.*, 2011); Xie changed the six-dimensional force sensor to integral pretightening double-layer parallel structure, improved the static and dynamic performance of sensor (Liu, 2016); Liu obtained the minimum range of the measurement branch and the corresponding parameters according to the working condition function model (Xie, 2011). The researchers have established a physical model of the sensor, by changing the structural parameters, using the optimal method to find the limit value and change trend of the observed target. At the same time, some researchers have found that the four-column elastomer has stronger antibias load capacity and better dynamic characteristics, which lays a foundation for the study of this paper. However, there is no quantitative analysis of the dynamic performance of the parameters of the structure.

The research content can be summarized as follows:

- We analyzed and studied the structural mechanism of the four-column elastomer and carried out the finite element simulation analysis by using solid works simulation software.
- We established the natural frequency model and modified the model according to the results of theoretical research.
- We carried out the optimal design of the four-column sensor and the sensor experiment, verified the accuracy of the established model and the improvement effect, completed the closed loop research of theory, simulation and experiment.

## 2 Modeling method

The modeling method is mechanism analysis method (Xu and Wen, 1990; Chen and Yuan, 1997), and the process is as follows:

- We analyzed the four-column elastomer and get the equivalent mode of the main structure.
- We studied the natural frequency of the equivalent model, stiffness distribution and mass distribution of four-column elastomer based on mechanism analysis method.
- We deduced and calculated the equivalent beam model, and combined the analysis of stiffness distribution and mass distribution of four-column elastomer, so as to established the natural frequency model of four-column elastomer.

### 2.1 Natural frequency theory

Natural frequency is defined as the specific frequency determined by the system itself when the structural system moves under external excitation (Xu *et al.*, 2014; Li *et al.*, 2017; Yang *et al.*, 2017). The natural frequency theory contains the following two important conclusions (Li *et al.*, 2017; Yang *et al.*, 2017), which are important theoretical basis for dynamic modeling of this subject:

- The natural frequency of an object is the inherent property of the object, which is determined by its own properties (such as quality and material) and unconcerned with external conditions (such as force state, constraint state and space state).
- The natural frequency of an object is only related to the stiffness distribution and mass distribution of the object, which is expressed as follows:

$$\omega^2 = \frac{k_p}{m_p} \tag{1}$$

$\omega$ is the natural frequency of the object, $k_p$ is the equivalent stiffness distribution of the object and $m_p$ is the equivalent mass distribution of the object.

### 2.2 Equivalent model analysis

When modeling a four-column elastomer, the four columns, the upper-end faces and the lower-end faces are integrated structures. The lower-end face can be constrained as a fixed end, and the upper-end face can be stressed as a free end. Each column can be simplified as one end supported and the other end free beam as Figure 1 shows. "A" indicates the lower face and "B" the upper face.

From the modal simulation image of the four-column elastomer in Figure 2, it can be seen that the modal analysis results of the lower end face of the four-column elastomer are displayed in

**Figure 1** Schematic diagram of equivalent beam model

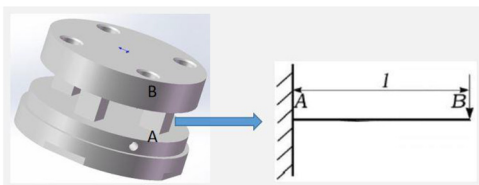


**Source:** Figure by author

**Figure 2** Modal and frequency analysis diagram of four-column elastomer

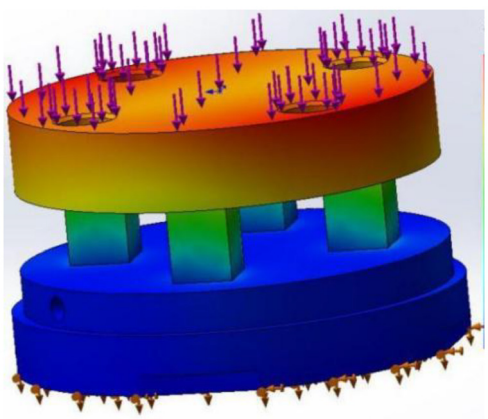

**Source:** Figure by author

blue, indicating that the lower end face of the elastomer does not participate in the frequency response process. The results of the modal analysis of the upper-end face are displayed in red, indicating that the frequency response of the upper-end face of the elastomer is complex and unstable, and cannot be used as the main object for the establishment of the natural frequency model of the four-column elastomer. The results of the four-column modal analysis are shown in green, indicating that the natural frequency response of the four columns of the elastomer is concentrated and stable, which dominates the frequency response analysis and can be used as the main object for the establishment of the natural frequency model of the four-column elastomer. As the final structure which applied the external load, the dynamic performance of the four-column elastomer is mainly related to the dynamic performance of the columns and the columns can be used as the main object for the establishment of the four-column elastomer natural frequency model.

We four identical columns are integrated with the upper and lower end faces by studying the overall structure form and component distribution state of the four-column elastomer. Under this structure form, the four columns are equivalent to "parallel" with each other. Refer to the structure parallel problem in Hooke's law (Zeng and Yang, 2024; Luo *et al.*, 2015; Ma, 1965), the stiffness of the overall parallel system is the sum of the stiffness of each parallel structure (Zeng and Yang, 2024; Luo *et al.*, 2015; Ma, 1965), the mass distribution of four-column elastomer can be regarded as the mass distribution of each column.

Based on the above analysis of stiffness distribution and mass distribution, it can be seen from the definition formula of natural frequency that the relationship between the overall natural frequency of four-column elastomer and each column is as follow:

$$\omega_n = \sqrt{\frac{k_p}{m_p}} = \sqrt{\frac{4k_0}{m_0}} = 2\sqrt{\frac{k_0}{m_0}} = 2\ \omega_0 \tag{2}$$

The natural frequency of the whole four-column elastomer is about twice that of each column.

$\omega_n$ is the natural frequency of the whole four-column elastomer, $\omega_0$ is the natural frequency of each column, $k_p$ is the overall stiffness distribution of the four-column elastomer, $m_p$ is the overall mass distribution of the four-column elastomer, $k_0$ is the stiffness distribution of each column and $m_0$ is the mass distribution of each column.

### 2.3 Establish the natural frequency model

The modeling method refers from the variational method of Hu Hai-chang (Hu, 1957), and is applied to the study of the natural frequency model of four-column elastomer column.

Make a linear elastic body vibrate naturally without external force, and the amplitude of the stress component is $\sigma_x$, $\sigma_y$,..., $\sigma_z$. The amplitude of the displacement component is $u$,$v$,$w$. The circumferential frequency is $\omega$, and the expression of motion is as follows:

$$\begin{aligned}
&\frac{\partial \sigma_x}{\partial x} + \frac{\partial \tau_{xy}}{\partial y} + \frac{\partial \tau_{xz}}{\partial z} + \rho\omega^2 u = 0\\
&\frac{\partial \tau_{xy}}{\partial x} + \frac{\partial \sigma_y}{\partial y} + \frac{\partial \tau_{yz}}{\partial z} + \rho\omega^2 v = 0\\
&\frac{\partial \tau_{xz}}{\partial x} + \frac{\partial \tau_{yz}}{\partial y} + \frac{\partial \sigma_z}{\partial z} + \rho\omega^2 w = 0
\end{aligned} \tag{3}$$

For the allowable state specified above, the extreme value of the formula in various allowable states corresponds to each order of natural frequency.

$$\begin{aligned}
\omega^2 &= ext\frac{\frac{1}{2}\iiint \rho(u^2+v^2+w^2)\,dxdydz}{\iiint V\,dxdydz}\\
&= ext\frac{\frac{1}{2}\omega^4\iiint \rho(u^2+v^2+w^2)dxdydz}{\iiint V(\sigma_x,\sigma_y,\ldots,\tau_{xy})dxdydz}
\end{aligned} \tag{4}$$

The minimum extreme value of the above formula is the first-order natural frequency of the object (Hu, 1957). And the natural frequencies of each order are the extreme values arranged from small to large (Hu, 1957).

After obtaining the natural frequency formula of general linear elastomer, we added the constraints of the columns' equivalent beam model, the natural frequency model of the four-column elastomer is obtained as follows:

$$\omega = 15.4\sqrt{\frac{EI}{\rho l^2}} \tag{5}$$

$\rho$ is the material density of four-column elastomer (unit: kg/m$^3$), $E$ is the elastic modulus (unit: Pa), $I$ is the section moment of inertia (unit: m$^4$) and $l$ is the height parameter of the elastomer.

According to the natural frequency definition, the overall natural frequency of the four-column elastomer body is about two times the natural frequency of each column. The formula of intrinsic angular frequency (unit: rad/s) is converted into the formula of intrinsic circular frequency (unit: Hz), and the rectangle of inertia of the section is expanded to obtain the natural frequency model of the four-column elastomer, which is shown in formula (6).

$$f = \frac{15.4}{\pi}\sqrt{\frac{Ebh^3}{12\rho l^4}} \tag{6}$$

Here $f$ is the natural frequency of the elastomer model; $b$ is the length parameter of the elastomer model; $h$ is the width parameter of the elastomer model.

## 3 Simulation and modified

We took the four-column elastomer with a measuring range of 20$t$ as the object of initial simulation research and comparison. The initial structural dimensions are shown in Table 1.

**Table 1** Initial structural parameters

| Structural parameters | 20t |
|---|---|
| Cross section $b \times h$ (mm) | 15 × 15 |
| The column height l (mm) | 20 |
| Radius of upper-end face R (mm) | 52.5 |
| Height of upper-end face H (mm) | 20 |
| The column spacing d(mm) | 65 |

**Source:** Table by author

The side parameter along the radial direction is the length parameter $b$, the side length parameter along the circumferential direction is the width parameter $b$ the column spacing $d$ is defined as the spacing between the centers of the columns on the opposite side. The struct parameters are shown in Figure 3.

### 3.1 Modify structure parameter

When some specific structure parameter changes, there is a great difference between the natural frequencies calculated by the model and simulation results, as Figure 4 shows.

**Figure 3** Structural parameters of four-column elastomer

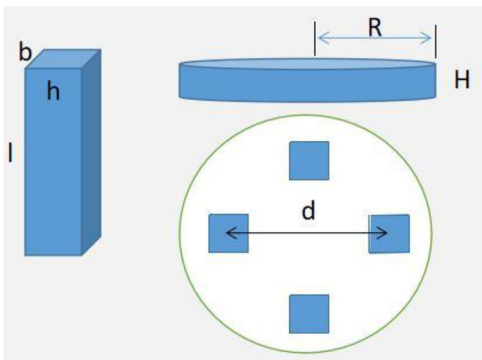


**Source:** Figure by author

Through the analysis of the stiffness distribution and the study on the effective structure parameter in the model. There is a correction formula under the condition when the width parameter and height parameter change.

$$b = h \tag{7}$$

$$\frac{1}{243.9 \times |1 - l_0| + 0.2725} \tag{8}$$

Expression (7) means that when the widening of the stiffness distribution changes, the length and width of the four columns are exchanged. After the change of the width parameter $h$ occurs, the stiffness distribution of the four columns of the four-column elastomer changes, that is, the widened column does not cause the change of the width parameter $h$ but causes the change of the length parameter $b$.

Figure 4 shows that the results of the uncorrected four-column elastomer natural frequency model are very different from the simulation results. With a lot of calculation and simulation results, it is found that there is a correction coefficient between the natural frequency calculated by the natural frequency model of the four-column elastomer and the natural frequency obtained by the simulation, and the coefficient changes with the height change value. The coefficient is formally as shown in expression (8).

The results in Figure 5 show that the calculation results of the dynamic mathematical model are more accurate and the correction effect of the model is good.

**Figure 4** (a) Comparison of uncorrected model when weight parameter change and (b) comparison of uncorrected model when height parameter change

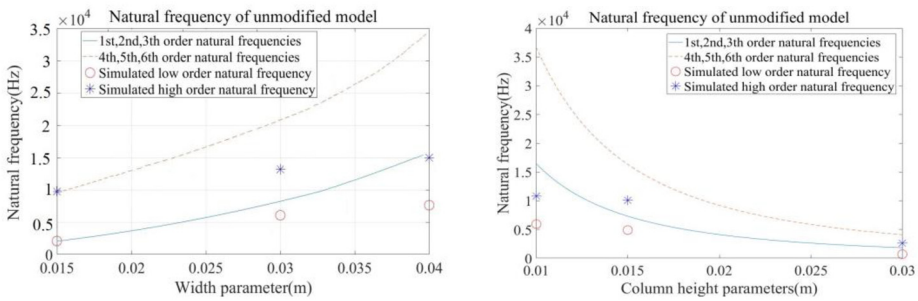


(a) (b)

**Source:** Figure by author

**Figure 5** (a) Comparison of corrected model when weight parameter change and (b) comparison of corrected model when height parameter change

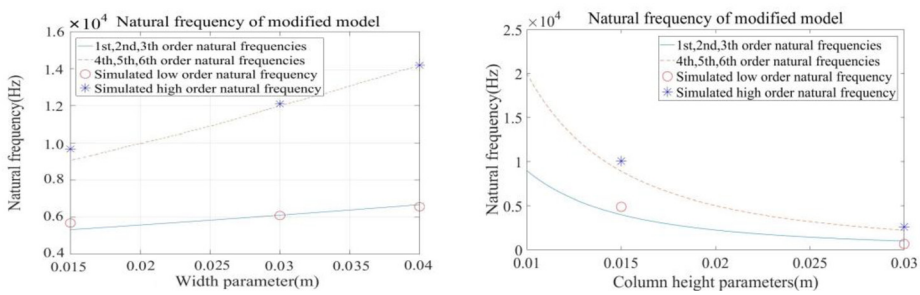


(a) (b)

**Source:** Figure by author

We studied the change of natural frequency when the column spacing $d$ changes. Combining simulation and theory, it can be seen that when the four columns move toward the center, the symmetrical structure of the four-column elastomer causes the stiffness distribution to change, and the effective length $b$ decreases by half the distance approaching. A corrective formula that reflects the change in the spacing between four columns of a four-column elastomer such as Shown in expression (9).

$$b = d - \frac{\Delta d}{2} \tag{9}$$

Here $b$ is the effective length, $d$ is the column spacing, $\Delta d$ is the changed spacing.

We studied the change of natural frequency when the column spacing $d$, the diameter $R$ and the height $H$ of the upper end face changes. The relationship between the natural frequency of the four-column elastomer and the stiffness distribution and mass is as follows:

$$\omega_1 = \sqrt{\frac{k_p}{m_1}},\ \omega_2 = \sqrt{\frac{k_p}{m_2}} \tag{10}$$

Here $\omega_1$ and $\omega_2$ are the original natural frequencies and the natural frequencies after the structural parameters of the upper face are changed, respectively. $k_p$ is the stiffness distribution of the four-column elastomer before and after the upper-end face structural parameters changing. $m_1$ and $m_2$ are, respectively, the mass of the original elastomer and the mass of the elastomer after the structural parameters of the upper face changing.

Therefore, the natural frequency relationship of the four-column elastomer before and after the structural parameters of the upper-end face change is as follows:

$$\omega_2 = \omega_2 \times \sqrt{\frac{m_1}{m_2}} \tag{11}$$

According to the research of theory and simulation results, the correction expression reflecting the change of column spacing $d$, the diameter $R$ and the height $H$ of the upper-end face is as follow:

$$\sqrt{\frac{4\rho_0 b_0 h_0 l_0 + \rho_0 \pi R_0^2 H_0}{4\rho bhl + \rho \pi R^2 H}} \tag{12}$$

Here $R$ and $H$ are respectively the radius and thickness of the upper end face of the elastomer. $b_0$, $h_0$, $l_0$, $R_0$ and $H_0$ are the initial structural dimensions.

The correction results are showed is Figure 6.

The results in Figure 6 show that the proposed correction methods make the calculation results of the model more accurate and verify the correction theory.

### 3.2 Summary

After the theory and simulation analysis, the changes of structural parameters related to the increase of natural frequency are as follows:

**Figure 6** (a) Comparison of corrected model when column spacing change; (b) Comparison of the upper-end face diameter change and (c) Comparison of the upper-end face height change

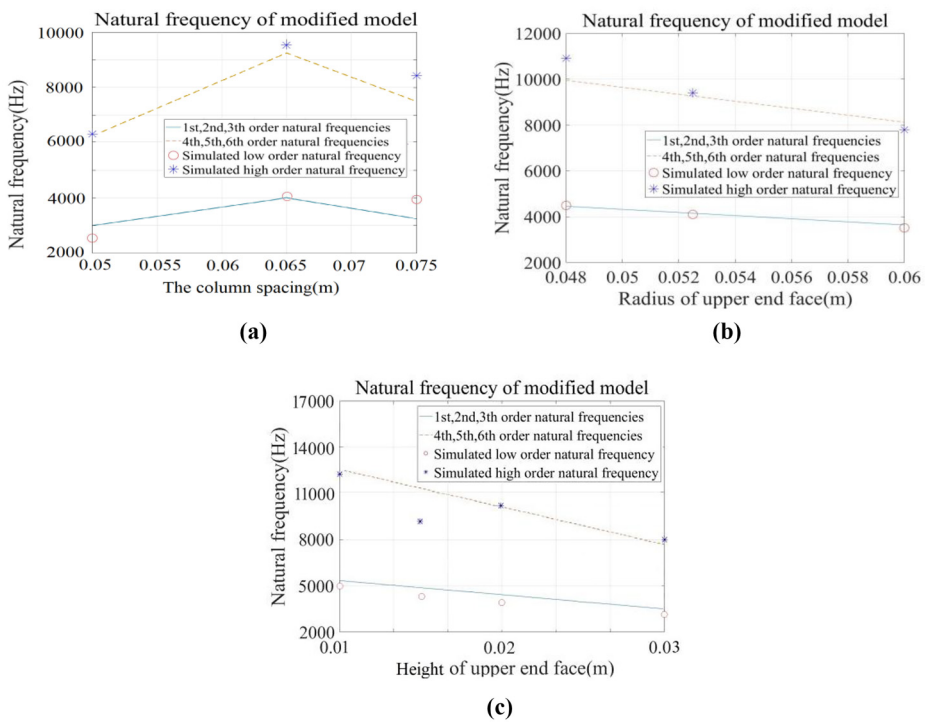


**Source:** Figure by author

**Table 2** Structural parameters of FC-10t and FC-20t

| Structural parameters | FC-10t | FC-20t | FC-10t (after optimization) | FC-20t (after optimization) |
|---|---|---|---|---|
| **Cross section $b \times h$ (mm)** | $8 \times 8$ | $11 \times 11$ | $8 \times 8$ | $11 \times 11$ |
| **The column height l (mm)** | 30 | 30 | 15 | 15 |
| **Radius of upper-end face $R$ (mm)** | 27.5 | 27.5 | 23 | 23 |
| **Height of upper-end face $H$ (mm)** | 18 | 18 | 7 | 7 |
| **The column spacing $d$ (mm)** | 27 | 27 | 18 | 21 |

**Source:** Table by author

**Figure 7** FD-3,000 dynamic and static load measuring instrument

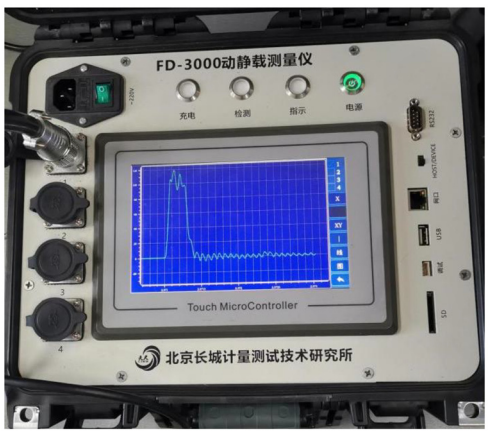


**Source:** Figure by author

**Table 3** FD-3,000 technical indicators

| Type specification | FD-3,000 |
|---|---|
| **Channel** | 4 |
| **Accuracy level** | Static force: 0.3 dynamic force 1 |
| **Unit select** | Force value, torque and other units |
| **Sampling frequency** | 500 kHz |
| **Input signal** | ±3.0 mV/V |
| **Working temperature** | −10 ~ 50°C |
| **Function** | Real time loading force curve display and data analysis |
| **Application** | Fatigue testing machine verification, static force verification, impact force test and electric power wrench calibration |
| **Overall dimension** | 320 × 280 × 140mm |
| **Weight** | 2.5 kg |

**Source:** Table by author

- lifting the column length parameter $b$;
- lifting the column width parameter $h$;
- reduce the column height parameter $l$;
- reduce the radius parameter $R$ of the upper-end face; and
- reduce the height parameter $H$ f the upper-end face.

The theoretical research conclusion is consistent with the simulation research conclusion.

According to the four-column elastomer natural frequency model analysis and correction, the complete four-column elastomer natural frequency model is obtained:

$$f = \frac{15.4}{\pi}\sqrt{\frac{Ebh^3}{12\rho l^4}} \times \frac{1}{243.9 \times |l - l_0| + 0.2725} \times \sqrt{\frac{4\rho b_0 h_0 l_0 + \rho\pi R_0^2 H_0}{4\rho bhl + \rho\pi R^2 H}} \quad (13)$$

The meaning of each parameter in the formula
$\rho$ is the material density of four-column elastomer (unit: kg/m$^3$);
$E$ is the elastic modulus (unit: Pa);
$b$ is the column length parameter (unit: m);
$h$ is the column width parameter (unit: m);
$l$ is the column height parameter (unit: m);
$R$ is the upper-end face radius parameter (unit: m);
$H$ is the upper-end face height parameter (unit: m); and
$b_0$, $h_0$, $l_0$, $R_0$ and $H_0$ are the initial structural dimensions (unit: m).

Under general conditions, expression (13) is the first three-order natural frequency model function expression. For the high-order conditions, the coefficients can also be taken as 2.232, 3.77, 6.63 and 12.25 (Zeng and Yang, 2024; Luo *et al.*, 2015; Ma, 1965). The equivalent beam mode is consistent with the column mode in the simulation study, which shows the correctness of the theoretical research.

## 4 Dynamic experiment

### 4.1 Purpose and steps

The aim of the experiment is to completed the closed loop research of theory, simulation and experiment.

Strictly speaking, the experimental object should be in a completely free state in the dynamic test and cannot be connected with other objects on any spatial coordinate axis, especially cannot have direct contact with the earth (AI and Cao, 2015). Under the existing experimental conditions, the experimental method can be realized by equivalent experiment, we placed the sensor system on the very soft and thick foamed plastic pads, which can be regarded as free state. This experimental method can realize the ideal dynamic test under the actual support conditions.

The experimental steps of four-column elastomer dynamic test are roughly divided into the following steps.

- We patched and encapsulated the existing or optimized four-column elastomer, and connected to the test instrument system.
- We placed the four-column elastomers on a thick foam plastic pad and placed the test instrument in the exclusive instrument box. Indirectly isolate the whole four-column sensor system from the earth.

- We keep the position and direction of knocks consistent, knock three to five–5 times, record the cycle time of its response waveform curve.
- We compared and analyzed the results of the model, simulation and experiment, analyzed the relative error, error sources and the limitations of research method.

### 4.2 Experiment and optimization design

The objects of experiment and structural optimization design are FC-10t sensor and FC-20t sensor. The optimal design schemes for the four-column elastomer are:

- We keep the length parameter $b$ and width parameter $h$ unchanged so as to keep the coupling characteristics, flexural modulus and sensitivity of four-column elastomer.
- We adjusted the column spacing to maximize the natural frequency of the four-column elastomer through simulation research.
- We reduced the height parameter $l$, reduced the height parameter $H$ of the upper end face and reduced the radius parameter $R$ of the upper end face. These three methods to improve the dynamic characteristics of the four-column sensor are constrained by engineering practice and boundary conditions.

Based on the above analysis, the structural parameters of FC-10t and FC-20t four-column elastomer before and after optimization design are shown in Table 2.

During the test, we connected the four-column sensor to the test instrument FD-3,000 dynamic and static load measuring instrument. The dynamic test performance of the test instrument is more than ten times that of the sensor and can collect the dynamic information of the sensor perfectly. Its shape and technical indicators are shown in Figure 7 and Table 3.

**Figure 8** (a) FC-10t four-column sensor and (b) FC-10t four-column sensor after structural optimization

(a) (b)

**Source:** Figure by author

The natural frequency and analysis of FC-10t four-column sensor before and after structural optimization are shown in Figure 8 and Tables 4 and 5.

The experiment results showed that, after the optimization, the natural frequency of FC-10t four-column elastomer increased 4081.2 Hz, the increase range is 49.38%.

We analyzed the experiment dynamic response waveform and extract the dynamic parameters, the rise time decreases, the peak time decreases slightly, the adjustment time remains basically unchanged and the overshoot time increases. The results showed that the rapidity and the amplitude frequency characteristics of the four-column elastomer FC-10t improve.

The natural frequency and analysis of FC-20t four-column sensor before and after structural optimization are shown in Figure 9 and Tables 6 and 7.

After optimized the FC-20t four-column sensor structural parameters, the experiment results showed that its natural frequency increased 3416.1 Hz and the increase range is 31.43%.

After optimization, the rise time decreases, the peak time decreases slightly, the adjustment time is basically unchanged and the overshoot increase. The dynamic performance improve, but its

**Table 5** Dynamic characteristic parameters of FC-10t before and after structural optimization

| Dynamic characteristic parameters | Before optimization | After optimization |
|---|---|---|
| **Rise time** | 1.00 s | 0.01 s |
| **Peak time** | 1.00 s | 0.93 s |
| **Adjustment time** | 2.99 s | 2.99 s |
| **Overshoot** | 0 | 947.2% |

**Source:** Table by author

**Figure 9** (a) FC-20t four-column sensor and (b) FC-20t four-column sensor after structural optimization

(a) (b)

**Source:** Figure by author

**Table 4** Result and analysis of FC-10t before and after structural optimization

| Sensor type | Experimental result (Hz) | Simulation result (Hz) | Model results (Hz) | Simulation relative error (%) | Model relative error (%) |
|---|---|---|---|---|---|
| **Before optimization** | 8264.5 | 9067.7 | 10,971 | 9.71 | 32.7 |
| **After optimization** | 12345.7 | 17,606 | 11637.4 | 42.6 | 6.09 |

**Source:** Table by author

**Table 6** Result and analysis of FC-20t before and after structural optimization

| Sensor type | Experimental result (Hz) | Simulation result (Hz) | Model results (Hz) | Simulation relative error (%) | Model relative error (%) |
|---|---|---|---|---|---|
| **Before optimization** | 10869.6 | 10,746 | 10177.5 | 1.04 | 6.36 |
| **After optimization** | 14285.7 | 22,076 | 13875.5 | 54.5 | 2.87 |

**Source:** Table by author

**Table 7** Dynamic characteristic parameters of FC-20t before and after structural optimization

| Structural parameters | Before optimization | After optimization |
|---|---|---|
| **Rise time** | 0.05 s | 0.02 s |
| **Peak time** | 5.51 s | 5.00 s |
| **Adjustment time** | 5.99 s | 5.99 s |
| **Overshoot** | 10.54% | 189.4% |

**Source:** Table by author

rapidity is lost. Overall, the amplitude frequency characteristics of the four-column elastomer FC-20t also improved.

## 5 Conclusions

We used the mechanism analysis method, the static and dynamic simulation analysis of finite element method and dynamic knocking method, studied and optimized the natural frequency and other dynamic properties of the four-column strain force sensor. We proposed the design theory of the four-column strain force sensor and researched the dynamic characteristics of four-column strain force sensor. We optimized the four-column sensors' structure and improved the dynamic performance based on the research theory. On the basis of not having a great impact on its static performance, the natural frequency of FC-10t sensor improved from 8264.5–12345.7 Hz, and the rapidity of the sensor improved slightly. The natural frequency of FC-20t sensor improved from 10869.6–14285.7 Hz, and the stability improved slightly. In general, the natural frequency and related dynamic performance improved more than 30%, and the optimization effect is verified by simulation and experiment, which completely verifies the research results and conclusions of the subject.

## References

Ai, W.G. and Cao, Z.X. (2015), "On the application of 'symmetry' in structural mechanics", *Real Estate Guide*, No. 16.

Cai, G.Q. (2019), "Application of photoelectric sensors in modern industrial production", *Electronic Testing*, No. 23, pp. 137-138 + 83, doi: 10.16520/j.cnki.1000-8519.2019.23.052.

Chen, X.B. and Yuan, Z.J. (1997), "Research on evaluation criteria and optimal design of multi-dimensional force sensor design", *Journal of Harbin Institute of Technology*, Vol. 29 No. 4, p. 5.

De Vries, P. (2018), "The presence of YHWH in exile according to the book of Ezekiel, with special reference to the meaning of the expression עַמְּךָ in Ezekiel 11: 16", *Old Testament Essays*, Vol. 31 No. 1, pp. 264-279.

Ding, J.Q. (2011), "Design of intelligent measurement and control system", *Knowledge Economy*, No. 2, p. 124, doi: 10.15880/j.cnki.zsjj.2011.02.055.

Guo, M.N. and Zhang, P. (2017), "Analysis on the application status of pressure sensing technology in modern medical research", *Electronic Journal of Integrated Traditional Chinese and Western Medicine Cardiovascular Disease*, Vol. 5 No. 22, pp. 14-16, doi: 10.16282/j.cnki.cn11-9336/r.2017.22.008.

Hu, H.C. (1957), "Two variational principles on the natural frequencies of elastomers", *Journal of Mechanics*, Vol. 1 No. 2, pp. 169-183.

Li, X.H., Huang, S.R. and Zhang, Q. (2017), "Natural frequency analysis of stator structure of permanent magnet synchronous motor for electric vehicle", *Chinese Journal of Electrical Engineering*, Vol. 37 No. 8, pp. 2383-2391.

Liu, W.Y. (2016), *Design and Experimental Study of Orthogonal Parallel Six Dimensional Force Sensor*, North China University of technology.

Luo, W., Dai, W., Ma, L., Huang, J., *et al.* (2015), "Improvement of Hooke's law exploration experimental device. Physical experiment".

Ma, R.Z. (1965), "Several problems about Hooke's law CNKI".

Ma, C., Zhu, G.F. and Liu, L.P. (2018), "Research progress on the application of biosensors in modern environmental pollution detection", *Rural Economy and Technology*, Vol. 29 No. 10, pp. 15-16.

Mu, L., Wang, X.W. and Fu, X.Y. (2020), "Classroom teaching reform of modern sensor technology and application", *Equipment Manufacturing Technology*, Vol. 12, pp. 235-237.

Sheng, G.L. and Huang, P. (2014), "Application of photoelectric sensors in modern industrial production", *New Technology and New Process*, Vol. 7, pp. 1-3.

Tang, H.B. (2016), "Analysis of robot and automation technology", *Scientist*, Vol. 4 No. 12, pp. 1-2.

Tang, Y. and Huo, L.G. (2020), "Research on the application of modern sensor technology in automotive electronics", *Electronic World*, No. 19, pp. 90-91, doi: 10.19353/j.cnki.dzsj.2020.19.041.

Tang, L., Xie, X.D. and Wang, J. (2011), "Research on advanced sensor materials and their applications", *Western China Science and Technology*, Vol. 10 No. 7, pp. 50-51.

Wu, J.L., Yang, M.L. and Liang, Y.X. (2011), "Design and optimization of four beam torque sensor", *Journal of Shaanxi Institute of Technology (NATURAL SCIENCE EDITION)*, Vol. 27 No. 4, pp. 1-6, doi:10.3969/j.issn. 1673-2944.2011.04.001.

Wu, Y.J., Liu, X.F., Lin, S. and Yuan, K.L. (2020), "Marine environment monitoring and modern sensor technology", *Information Recording Materials*, Vol. 21 No. 10, pp. 29-30, doi: 10.16009/j.cnki.cn13-1295/tq.2020.10.018.

Xie, X.W. (2011), *Development and Performance Analysis of an Integral Preloaded Double-Layer Parallel Six Dimensional Force Sensor Prototype [D]*, Yanshan University.

Xu, K.J. and Wen, M. (1990), "Research on mathematical model of sensor", Journal of Hefei University of Technology (NATURAL SCIENCE EDITION).

Xu, G., Gong, Q.W., Guan, Q.Y., Li, W. and Feng, R.F. (2014), "Fault phase selection method using traveling wave natural frequency and atomic energy entropy", *Power Grid Technology*, Vol. 38 No. 6, pp. 1688-1693.

Xxxx, X. (2019), "Action plan for accelerating the development of sensor and intelligent instrument industry", *China Metrology*, No. 7, pp. 21-24, doi: 10.16569/j.cnki.cn11-3720/t.2019.07.009.

Yang, H.K., Che, A.L. and Li, Y.M. (2017), "Influence of initial effect of concentrated static load on natural frequency of fixed beam", *Journal of Applied Mechanics*, No. 6, pp. 1055-1060 + 1216.

Ye, Y., Wang, Y.S. and Zhu, J.H. (2001), "Application and development of chemically sensitive materials", *Journal of Naval Engineering University*, No. 4, pp. 108-111+116.

Zeng, X.Y. and Yang, Z.C. (2024), "Study on Hooke's law yield condition and strengthening effect of biaxial tension of anisotropic titanium plate. VIP, one thousand nine hundred and ninety-two".

Zhang, W., Zhang, Y., Zhang, Z.M., Hu Gang. and M., Feng. (2012), "Research on dynamic measurement system of strain gauge force sensor", *Shipbuilding Engineering*, Vol. 34 No. S1, pp. 67-69.

Zhao, B. (2020), "Research on application and development of modern measurement and control technology", *Equipment Management and Maintenance*, Vol. 4, pp. 138-139, doi: 10.16621/j.cnki.issn1001-0599.2020.02d.75.

Zhao, Y.M., Chen, K.X., Chai, J.X. and Wang, L.L. (2017), "A four column high precision resistance strain force sensor", *Measurement Technology*, Vol. 37 No. 0z1, pp. 129-133.

Zhou, S.H. and Luo, H. (2015), "Design of modern sensor conditioning circuit based on new special operational amplifier", *Electronic Quality*, No. 1, pp. 40-43.

Zhou, S.H., Long, Y.J. and Tu, Y.C. (2013), "Misunderstandings and countermeasures in the design of modern sensor preamplifiers", *Journal of Xinyang Normal University (NATURAL SCIENCE EDITION)*, Vol. 26 No. 4, pp. 592-595.

## Further reading

Jiang, K.Y. (2016), "Strengthening and application of the concept of symmetry in structural mechanics", *Three Gorges Higher Education Research*, No. 2, pp. 63-67.

Wei, R. *Research on Dynamic Test Excitation Method of Multi-Dimensional Force Sensor*, Anhui University of engineering.

Wei, K., Wang, P. and Niu, P.B. (2019), "Study on the influence of rail modal order on wheel rail high frequency dynamic response of high-speed railway", *High Speed Railway Technology*, Vol. 10 No. 1, pp. 1-5.

## Corresponding author

**Yinming Zhao** can be contacted at: zhaoyinming@cimm.com.cn